ONLINE RESOURCE 2
MULTIVARIATE SPSS ANALYSIS

Ceramic Production and Exchange in the Chavín Heartland: An Archaeometric Study from Canchas Uckro (1100-800 BCE), Ancash, Perú
Submitted to: *Archaeological and Anthropological Sciences*

Rachel Johnson[a*], Bebel Ibarra Asencios[b], Jason Nesbitt[a], Julia Sjödahl[a], and MinJoo Choi[a]

[a]Tulane University, Department of Anthropology, New Orleans, LA, USA
[b]Pontificia Universidad Católica del Perú, Departamento de Humanidades, San Miguel, Lima, Perú
*Corresponding Author: rjohns35@tualne.edu

Statistical analysis of pXRF compositional data was conducted using Statistical Package for the Social Sciences (SPSS) to test hypotheses based on reflective microscopic data and prior archaeological excavations (e.g. Ibarra Asencios 2009, 2021, Nesbitt et al. 2020, 2021, 2023) Discussion of the dataset documents the step-by-step statistical process, addressing elimination of variables and contextualizing final interpretations. All tables, graphs, and charts supporting the arguments made in this article are included in this appendix.

Canchas Uckro

Tested Hypotheses:

1. **The initial DinoLite study highlighted general homogeneity within the assemblage. It is expected that geochemical data will identify a limited number (1-2) of technological traditions associated with local production.**
2. **A small number of artifacts exhibit significant technological differences, suggesting Canchas Uckro was embedded within regional and inter-regional exchange networks, typical of economic and social interaction c. 1150-650 BCE. Outlier sherds are expected to cluster away from local production, supporting a non-local origin.**
3. **A high proportion of decorated sherds at Canchas Uckro exhibit Waira-jirca design motifs (~10%). As a suspected import, Waira-jirca style sherds will group separately from other technological styles.**

Part I. Preliminary Hierarchical Cluster Analysis (HCA)

Cleaned pXRF data (n=55) were clustered using multiple clustering algorithms. The cluster based on between-groups linkage (average distance between pairs of cases) and squared Euclidian distance – which places increasingly greater emphasis on cases further away from group center, suggests that most artifacts from Canchas Uckro likely group together in a single large cluster (dark blue), alongside a secondary cluster (green), two smaller clusters (orange and red), and several outliers. A cluster using ward's method (which can mask outliers) produces approximately the same results, though it notably splits the single large cluster into several smaller groups. Related to technological differences, corresponding to the dominant production practice, featuring intrusive volcanic sediments and explosive volcanic tuffs, as well as "nearby" production styles, dominated by slate, schist, and graphite, all of which are available within the broader Conchucos region, accompanied by clear stylistic outliers. *These preliminary findings suggest Canchas Uckro was integrated within both regional and interregional exchange networks*.

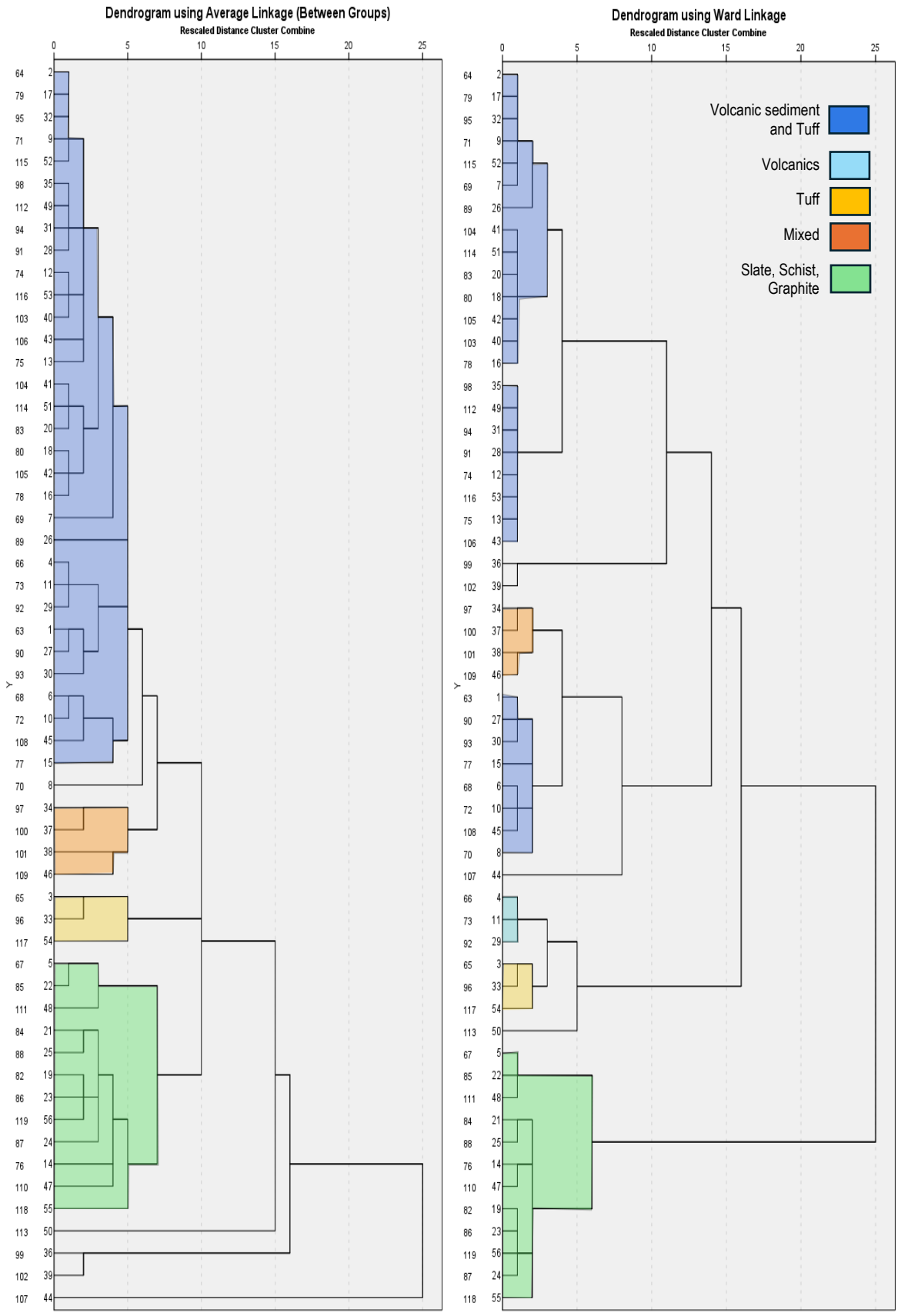

Figure D-1. Preliminary clusters of Canchas Uckro pXRF data.

Table D-1. KMO and Bartlett's Test, Canchas Uckro PCA Attempt 1

Kaiser-Meyer-Olkin Measure of Sampling Adequacy.		.517
Bartlett's Test of Sphericity	Approx. Chi-Square	616.627
	df	136
	Sig.	**<.001**

Part II: Principal Component Analysis (PCA)

To apply PCA, the data must meet a few assumptions. First, the number of cases should ideally outnumber the analyzed variables 5 to 1 (Costello and Osborne 2005; Hair et al. 2010) .Given the total available sample size (n=56) and the high number of elemental variables measured, the number of variables should be systematically reduced to improve analytical outcomes. During data cleaning, variables exhibiting greater than 20% error were removed from the dataset to improve the reliability of the geochemical findings, resulting in the 17 elemental variables utilized in PCA.

In the first attempt at PCA, the KMO value of 0.517 is poor (KMO value should ideally >0.700, indicative of a sufficient sample size, and at minimum >0.500; Costello and Osborne 2005). The anti-image matrix of sampling correlation indicates measures of sampling adequacy are the lowest for: Si, P, K, Ga, As, Rb, using 0.400 as an arbitrary cut off. These elements were eliminated from further analyses to improve sampling adequacy.

Table D-2. KMO and Bartlett's Test, Canchas Uckro PCA Attempt 2

Kaiser-Meyer-Olkin Measure of Sampling Adequacy.		**.720**
Bartlett's Test of Sphericity	Approx. Chi-Square	285.388
	df	55
	Sig.	**<.001**

A second KMO (Kaiser-Meyer-Olkin) test for sampling adequacy indicates the sample is large enough to conduct PCA (Table E-2), though it should be noted that statistically, this value is still considered average. Bartlett's Test of Sphericity was also significant (P<0.001), indicating that variables are correlated and can be used in factor analysis.

Review of the scree plot inflection point indicates there should be two components based on PCA of the 11 utilized elements. Applying the Kaiser-Guttman rule, which drops components with eigenvalues less than 1, suggests four principal components explain most data variation (71.9%). Most of the variation is loaded on Component 1 (35.5%), while Component 2 loads 17.3%, Component 3 loads 14.0%, and Component 4 loads 9.6% of the assemblage compositional variation.

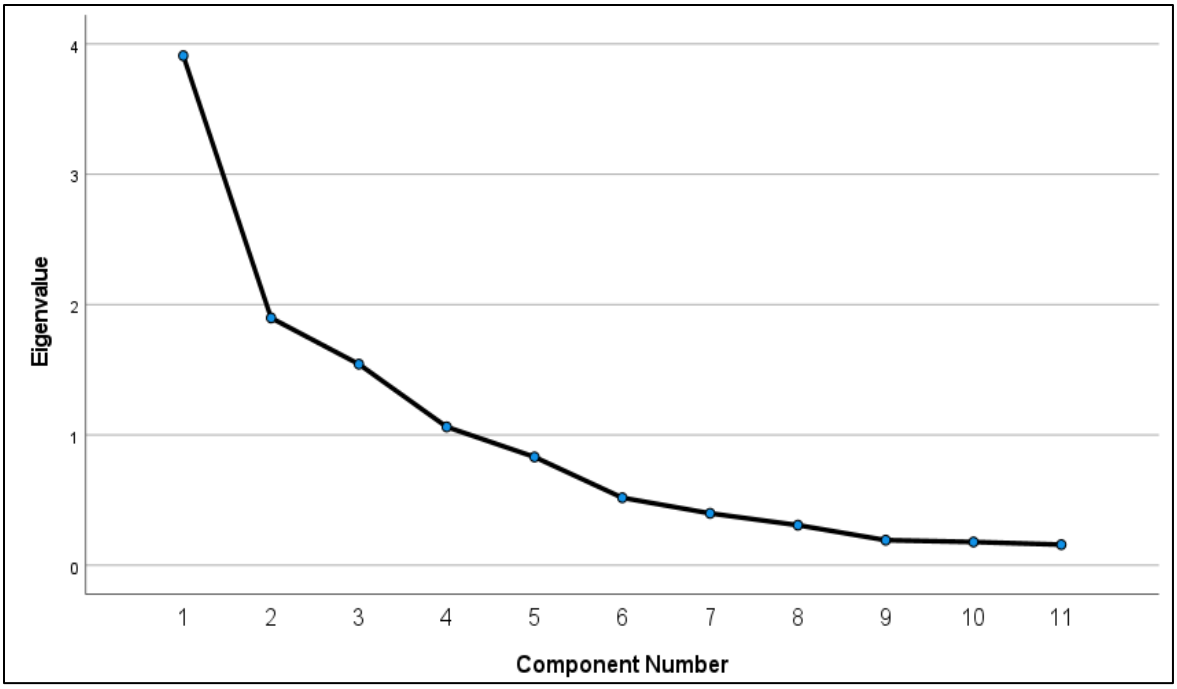

Figure D-2. Screen Plot, Canchas Uckro PCA

Table D-3. Table of Total Variance Explained, Canchas Uckro PCA

	Initial Eigenvalues			Extraction Sums of Squared Loadings		
Component	Total	% of Variance	Cumulative %	Total	% of Variance	Cumulative %
1	3.910	35.549	35.549	3.910	35.549	35.549
2	1.898	17.256	52.805	1.898	17.256	52.805
3	1.543	14.031	66.837	1.543	14.031	66.837
4	1.062	9.654	76.491	1.062	9.654	76.491
5	.831	7.556	84.047			
6	.518	4.712	88.759			
7	.399	3.623	92.383			
8	.308	2.799	95.182			
9	.193	1.752	96.934			
10	.179	1.625	98.559			
11	.159	1.441	100.000			

Table D-4. Promax component correlation matrix, Canchas Uckro PCA

Component	1	2	3	4
1	1.000	**.323**	.103	.060
2	**.323**	1.000	.127	.000
3	.103	.127	1.000	-.066
4	.060	.000	-.066	1.000

The data matrices were rotated to maximize factor loading. Orthogonal (e.g. varimax, quartimax, equamax) and oblique (promax) rotations were applied to the dataset to evaluate which rotation best differentiated the principal components.

Table D-5.Promax and varimax rotated component matrices, Canchas Uckro PCA.

Promax Rotated Component Matrix

	Component			
	1	2	3	4
Al*	**.328**	**.895**	-.063	.043
S	.283	.266	-.040	**.696**
Ca	**-.809**	-.110	-.084	**.362**
Ti	.290	**.931**	.188	-.041
Fe*	.226	**.727**	**.427**	.035
Mn	-.203	.104	**.833**	-.263
Zn*	**.749**	.110	.264	**.362**
Sr*	**-.884**	**-.436**	.022	-.171
Y*	**.877**	**.401**	-.088	.004
Zr*	**.302**	**.327**	.272	**-.713**
Ba*	**-.549**	-.183	**-.678**	-.043

Varimax Rotated Component Matrix

	Component			
	1	2	3	4
Y	**.848**	.286	-.153	-.034
Sr*	**-.843**	**-.320**	.079	-.134
Ca	**-.833**	.015	-.026	**.397**
Zn*	**.746**	-.008	.249	**.335**
Ti	.124	**.919**	.108	-.044
Al	.178	**.885**	-.141	.034
Fe*	.083	**.708**	**.370**	.038
Mn	-.260	.108	**.829**	-.240
Ba*	**-.513**	-.082	**-.653**	-.031
Zr	.261	.279	.200	**-.722**
S	.233	.240	-.034	**.686**

The component correlation matrix, extracted by Promax rotation, indicates some degree of component correlation between Factors 1 and 2, exceeding the recommended 0.32 correlation threshold (Tabachnick and Fidell 2007:646). Subsequent comparison with the orthogonal varimax rotation indicates the Varimax rotation loads individual variables more independently when compared to the Promax rotation. The bolded numbers indicate values >.30, which can be interpreted as “significant” loading (Kline 2014:52–53). The Varimax rotation provides better separation of the data with only four complex variables, that is a variable with loadings of 0.3 or higher on multiple factors. The Promax rotation, by comparison, 7 of the 11 analyzed variables are complex. Ideal component matrices should follow “simple structure”, in that each pair of

components should have variables with significant loadings (>0.3) on one component and near zero (between ±0.1) on the other, while minimizing the number of complex variables (i.e. variables loading at >0.3 on multiple components) (Tabachnick and Fidell 2007). The Varimax rotation was therefore selected to improve the interpretability of results.

In the Varimax component matrix, yttrium, calcium, and zinc load heavily on component 1, alongside an inverse relationship with strontium and barium. Titanium, aluminum, and iron load on Component 2, as well as the complex variable strontium. Component 3 loads heavily with manganese and iron, along with an inverse relationship with barium, while Component 4 loads calcium, zinc, and sulfur, and inversely loads zirconium.

The varimax-rotated Principal Components results were integrated with the findings of petrographic analysis to assess if geochemical differences correspond to technological differences. Review of the Component 1 v. Component 2 scatterplot shows generally good separation. Slate, graphite (green cluster) and schist (light blue cluster) show enriched concentrations of Ti, Al, Fe (Component 2 elements) relative to other ceramics. The geochemical overlap of slate and graphite temper ceramics is not unexpected. Prior study of slate tempers identified multiple potential sources, each with a distinct carbon content (Druc 2001). Outside of overlaps with the dominant technological variety ("felsic sed."), there is good clustering of petrographically-identified types (e.g. "Tuff" and "Alt. Volcanic"). The altered intrusive tempered sherds (dark blue cluster) notably create their own group; these cases repeatedly separate from the Canchas Uckro assemblage in preliminary HCA, pointing to a non-local origin for these sherds (Artifact # 99 and 102).

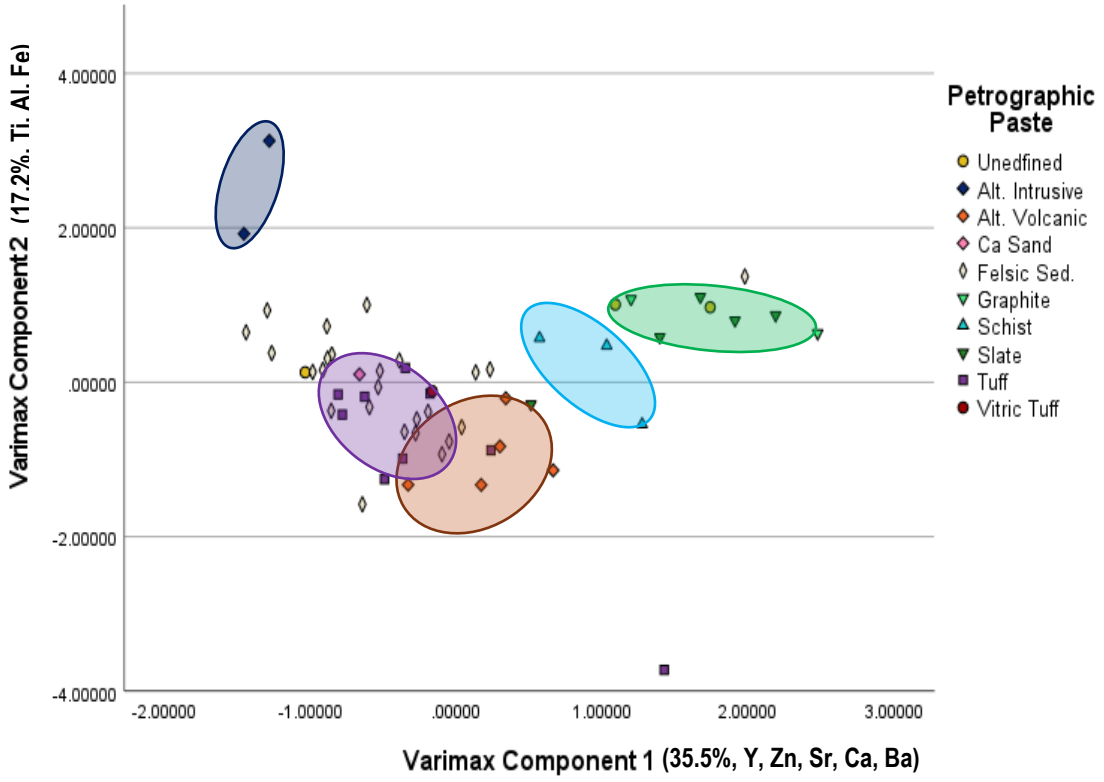

Figure D-3. Scatterplot of varimax Component 1 and 2, Canchas Uckro PCA

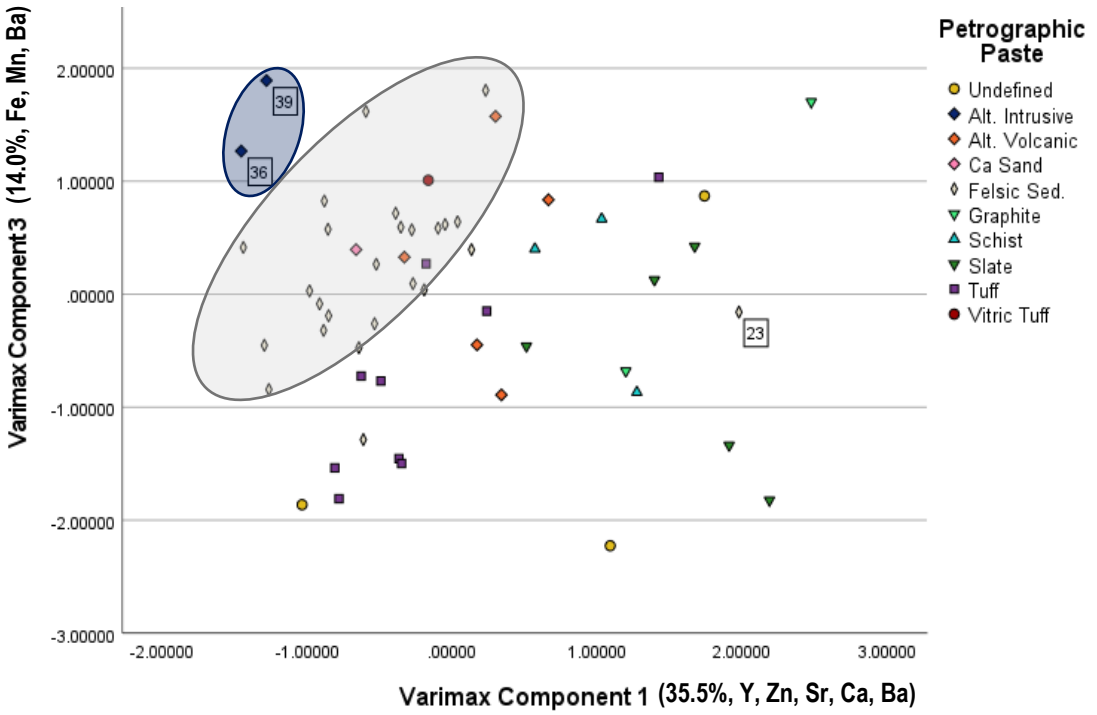

Figure D-4. Scatter plot of varimax Component 1 and 3, Canchas Uckro PCA

The Component 1 v. Component 3 graph highlights similar trends. Most notably, this graph illustrates some degree of separation between the dominant technological type (light gray cluster) and the remainder of the sample assemblage, with the notable exception of one sherd (Case 23) that may warrant further investigation. In general, these materials show relatively low concentrations of elements loaded on Component 1, increasing in proportion to the concentration of elements loaded on Component 3 (Fe, Mn, Ba).

Part III: Hierarchical Cluster Analysis (HCA)

HCA was repeated on the PCA components, using several clustering algorithms to optimize visualization of data differences. The first dendrogram highlights the clusters observed during analysis. The between-groups linkage dendrogram shows two primary clusters (blue and green), and several potential subclusters. The larger of the two clusters (blue) is likely associated with the dominant community of practice, expected to represent local production and local raw materials. Linking the clusters with preliminary RLM technological types shows the second cluster (green) is associated almost exclusively with metamorphic pastes types. Because the geology surrounding Canchas Uckro does not contain a high quantity of slates and schists, these sherds may represent exchange within the broader Puccha Valley, as schists outcrop with the Marañon Group near the confluence of the Puccha and Marañon Rivers, while slates and graphite are more typical of shashal temper, associated with the Chicama Formation (Druc 2001, 2005).

Overall, HCA of the PCA factors roughly parallel the results of preliminary HCA. Review of the various clustering algorithms suggests that Average Linkage (between-groups linkage) presents the best representation of the data.

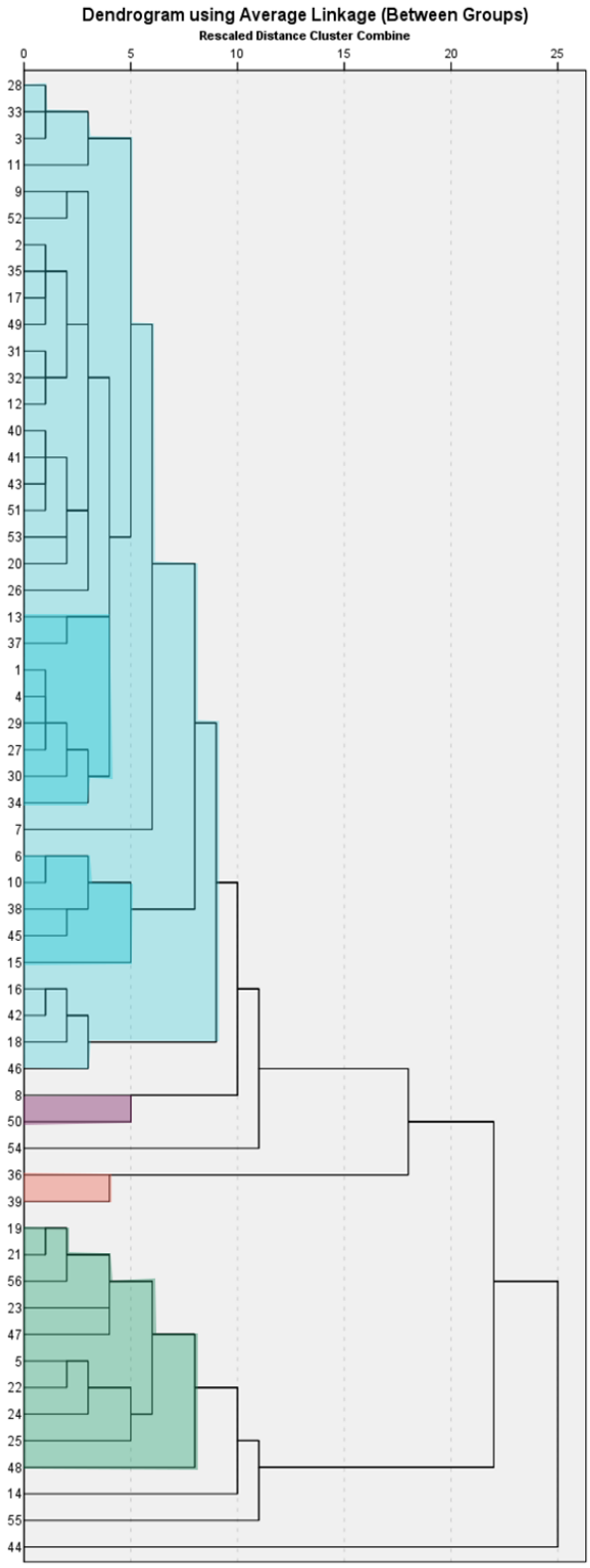

Figure D-5. Average linkage dendrogram highlighting the clusters identified by PCA and HCA.

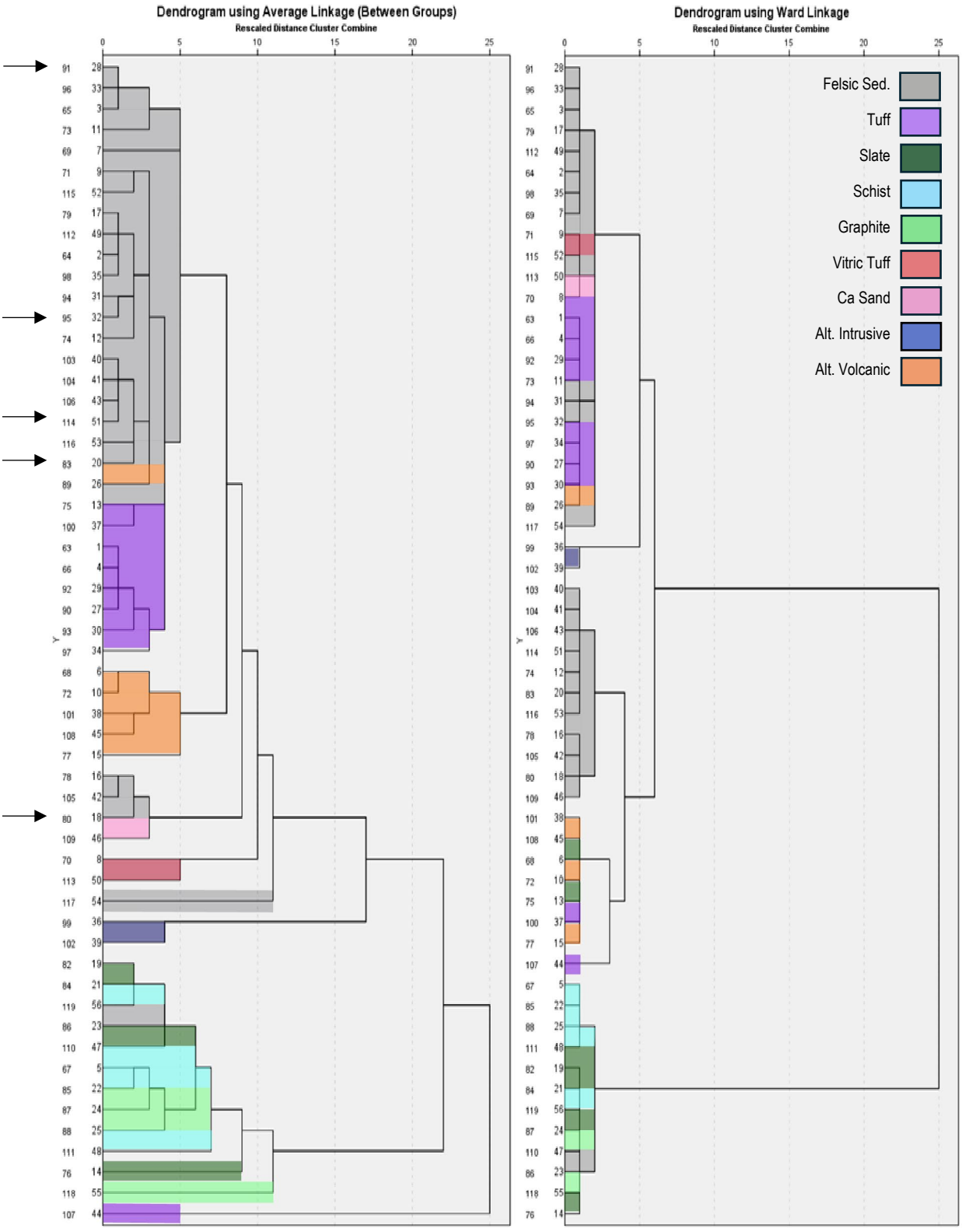

Figure D-6. Hierarchical clusters, Average Linkage (left) and Ward's Method (right), of PCA components, color-coded by petrographic technological group; black arrows denote Waira-jirca sherds in the local technological tradition.

The clusters were subsequently linked to petrographic groups to evaluate grouping trends (Figure E-6). Both the between-groups linkage and Ward's method clustering algorithms identify the same metamorphic group. However, Ward's Method appears to obscure outliers and produces clusters with a higher proportion of mixed technological types compared to the Average-Linkage cluster.

The petrographic groups highlighted here can be linked to different parts of the landscape based on the composition of the identifiable rock and temper inclusions:

Gray:	Felsic Intrusive; "Local" assemblage
Purple:	Volcanics; "Nearby" or "Local" assemblage
Orange:	Altered Volcanics; possibly of Huallaga origin?
Dark Green:	Slate, "Nearby" Chicama Formation
Light Green:	Graphite, "Nearby" Chicama Formation
Light Blue:	Muscovite Schist, "Nearby", Manrañon Complex
Pink:	Calcareous Sand, Non-Local
Red:	Intermediate Intrusive, Non- Local

The gray cluster represents the dominant technological tradition within the Canchas Uckro assemblage, representing the local community of practice. Of note, approximately half of the analyzed waira-jirca sherds geochemically and technologically cluster with this dominant technological practice, indicating they were made using local raw materials. **This finding disproves the initial hypothesis that Waira-jirca was exclusively an imported ceramic style.**

Volcanic tuff-tempered sherds may represent a second local community of practice. These materials generally cluster with the dominant assemblage, which may point to clay similarities with tempering differences. Technologically, they can be distinguished from the felsic sedimentary group primarily through the inclusion of tuff fragments. Though volcanic tuffs are not present in geologic maps or reported in reports in the immediate vicinity of the site (Wilson, Molina, et al. 1995; Wilson, Reyes Rivera, et al. 1995), rhyolitic tuff has been reported from near Antamina, a large copper-zinc mine just 12 km south of Canchas Uckro. This area is notably near the path of the Qhapaq Ñan, the Inka road, suggesting that this tuff, or perhaps another nearby outcrop, may be the source of tuff temper. Similar raw materials are also reported in the vicinity of Chavín de Huántar within the upper Mosna drainage (Druc 2004), potentially pointing to additional intraregional ties.

Some potential outliers, like the Intermediate Intrusive (red) cluster, remain relatively consistent across all analyses, supporting a non-local origin. *In sum, these findings suggest at least two communities of practice were actively participating in pottery production at Canchas Uckro, supported by both intra- and interregional exchange.*

Part IV: Mahalanobis Distance and Identifying Outliers

Given the results of HCA and the various potential outliers, Mahalanobis distance was used to identify outliers in the sample. The sample groups were split into two groups, paralleling the two main compositional groups identified in HCA. Mahalanobis distance was calculated for each of the two groups original elemental concentrations. The threshold probability of group membership was set to <5%, meaning that individual cases with a less than 5% probability of being group members were identified as outliers. In this study, two samples (CU102 and CU107) were identified as definitive outliers. Both samples are associated with Group 1, the cluster associated with local production.

Table D-6. Mahalanobis Distance and associated group probabilities; outliers are bolded.

	ID	CLUSTER	MAH_DIS	MAH_PROB
GROUP 1	63	1	1.51758	0.82352
	64	1	1.42861	0.83921
	65	1	3.29686	0.50943
	66	1	3.82098	0.43077
	68	1	0.8384	0.93323
	69	1	3.02833	0.5531
	70	3	1.29763	0.86178
	71	1	0.72649	0.94802
	72	1	1.24671	0.87035
	73	1	5.45499	*0.24371*
	74	1	0.75977	0.94376
	75	1	0.27192	0.99155
	77	1	1.968	0.74164
	78	1	0.22579	0.99409
	79	1	1.8206	0.76871
	80	1	1.81058	0.77055
	83	1	0.9871	0.91175
	89	1	3.42834	0.48886
	90	1	3.83723	0.42848
	91	1	4.56712	0.33466
	92	1	5.01853	*0.2854*
	93	1	3.69648	0.44864
	94	1	3.18622	0.52716
	95	1	2.20316	0.69845
	96	1	3.66126	0.45379
	97	1	2.62686	0.62207
	98	1	1.58164	0.81209
	99	4	7.42366	*0.11512*
	100	1	0.76121	0.94357
	101	1	3.65926	0.45408
	102	4	13.33473	**0.00975**
	103	1	1.81668	0.76943
	104	1	1.38307	0.84713
	105	1	0.95525	0.9165
	106	1	5.01142	*0.28613*
	107	5	15.05456	**0.00459**
	108	1	2.24598	0.69062
	109	1	3.67392	0.45193
	112	1	2.70775	0.60786
	113	3	1.41946	0.84081
	114	1	0.70739	0.95042
	115	1	1.58967	0.81065
	116	1	0.3998	0.98249
	117	6	5.549	*0.23546*
GROUP 2	67	2	0.12193	0.9982
	76	2	0.73194	0.9473
	82	2	1.37332	0.8488
	84	2	1.80327	0.7719
	85	2	0.39951	0.9825
	86	2	1.47232	0.8315
	87	2	0.5392	0.9696
	88	2	0.44647	0.9785
	110	2	1.05274	0.9017
	111	2	0.61008	0.9619
	118	7	2.30976	0.679
	119	2	1.13945	0.888

Part V: Discriminant Function Analysis (DFA)

To verify group membership, this analysis input the 2 main clusters and 5 outlier groups identified in the Average-Linkage HCA as grouping variable and the elements utilized in the final statistical procedure as the independent variables. Group size was not assumed to be equal, based on the initial findings of HCA. DFA employed a stepwise Mahalanobis distance methodology, setting the threshold of group membership at >5%. Of note, the tuff-tempered group and altered volcanics group, which were observed to be technologically distinct, do not separate from the overall Group 1 cluster in this analysis.

Table D-7. Eigenvalues of Discriminant Functions. Values associated with strong Canonical Correlation are bolded.

Function	Eigenvalue	% of Variance	Cumulative %	Canonical Correlation
1	10.117[a]	54.2	54.2	.954
2	4.754[a]	25.4	79.6	.909
3	2.185[a]	11.7	91.3	.828
4	1.130[a]	6.0	97.3	.728
5	.335[a]	1.8	99.1	.501
6	.162[a]	.9	100.0	.373

Table D-8. Wilks' Lambda for Discriminant Function Analysis; Significant values (<0.05) are bolded; Functions 1-5 best explain differences between different groups.

Test of Function(s)	Wilks' Lambda	Chi-square	df	Sig.
1 through 6	.001	306.045	54	**<.001**
2 through 6	.017	192.845	40	**<.001**
3 through 6	.095	110.602	28	**<.001**
4 through 6	.303	56.162	18	**<.001**
5 through 6	.645	20.630	10	**.024**
6	.861	7.050	4	.133

Table D-9. Standardized Canonical Discriminant Function Coefficients. Bolded values (>∓0.50) indicate elements that most strongly impact the discriminant score of each function.

	Function					
	1	2	3	4	5	6
Al	-.115	-.234	.190	**.808**	.071	**.697**
Ca	.410	**-.562**	**1.358**	-.274	.244	-.235
Ti	**-1.033**	-.259	**-.745**	.005	.311	**-.629**
Fe	.011	**-.571**	.071	-.474	-.233	.247
Zn	.126	**.552**	-.293	.262	**.883**	.434
Sr	**.883**	.236	**-.667**	-.158	.367	.280
Y	.121	**.682**	**.507**	**-.625**	.163	-.256
Zr	.402	.178	**1.132**	.437	-.398	.244
Ba	.189	**.706**	-.296	**.757**	.138	-.408

Table D-10. Structure Matrix, Canchas Uckro DFA

	Function					
	1	2	3	4	5	6
Sr	**.536***	-.301	-.260	.098	.089	-.062
Ti	-.426*	-.303	-.031	.198	.209	-.199
Y	-.426	**.499***	**.334**	-.274	.120	.027
Fe	-.261	-.310*	-.056	-.128	-.081	.276
Mn[b]	-.042	-.287*	-.037	-.169	.000	.283
Al	-.324	-.169	.219	**.464***	.246	.261
Zn	-.182	.233	.025	-.159	**.590***	**.501**
Ca	**.307**	-.471	.297	.120	**.587***	-.471
Zr	-.076	.083	.167	.194	-.435*	.295
Ba	.164	.039	-.045	**.526**	.063	-.610*
Ga[b]	.017	.020	-.022	.107	.187	.248*

*. Largest absolute correlation between each variable and any discriminant function

b. This variable not used in the analysis.

The Structure Matrix represents pooled within-groups correlations between discriminating variables and standardized canonical discriminant functions. These correlations are comparable to PCA factor loadings. Correlations >0.3 are considered potentially significant and are bolded in the table.

Table D-11. Functions at Group Centroids: the means of the discriminant function scores by predetermined canonical variables for the elemental data using Average-Linkage clustering and squared Euclidian distance.

	Function					
Predicted Group for Analysis 1	1	2	3	4	5	6
1	1.436	-.184	-.388	.362	-.026	.052
2	-4.883	1.805	.346	.125	.214	-.232
3	2.275	-2.122	3.681	-1.904	1.976	.421
4	-5.174	-8.740	-.596	-1.539	-.683	-.451
5	3.945	5.203	-4.357	-5.942	-.196	-.367
6	6.628	2.153	6.969	-.804	-1.929	-1.199
7	-5.636	1.523	2.154	-1.501	-1.839	2.214

Unstandardized canonical discriminant functions evaluated at group means

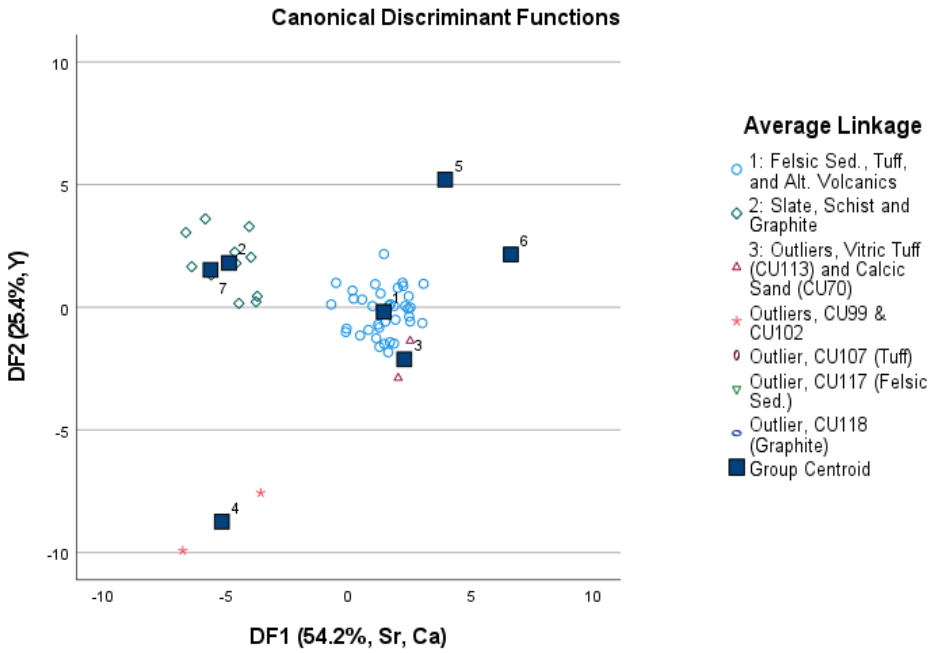

Figure D-7. Scatterplot of DF 1 vs. DF 2, Canchas Uckro, DFA

DFA groups 94.6% (n=53 of 55) of cases with the clusters created by PCA and HCA analyses, indicating the initial statistical analyses effectively grouped the dataset, establishing a "local" geochemical signature, identifying both a "nearby" metamorphic-temper-based technological style and several potential outliers.

Table D-12. DFA Classification Results, Canchas Ucrko

			Predicted Group Membership							
		Predicted Group for Analysis 1	1	2	3	4	5	6	7	Total
Original	Count	1	38	0	0	0	0	0	0	38
		2	0	11	0	0	0	0	0	11
		3	2	0	0	0	0	0	0	2
		4	0	0	0	2	0	0	0	2
		5	0	0	0	0	1	0	0	1
		6	0	0	0	0	0	1	0	1
		7	0	0	0	0	0	0	1	1
	%	1	100.0	.0	.0	.0	.0	.0	.0	100.0
		2	.0	100.0	.0	.0	.0	.0	.0	100.0
		3	100.0	.0	.0	.0	.0	.0	.0	100.0
		4	.0	.0	.0	100.0	.0	.0	.0	100.0
		5	.0	.0	.0	.0	100.0	.0	.0	100.0
		6	.0	.0	.0	.0	.0	100.0	.0	100.0
		7	.0	.0	.0	.0	.0	.0	100.0	100.0

a. 96.4% of original grouped cases correctly classified.

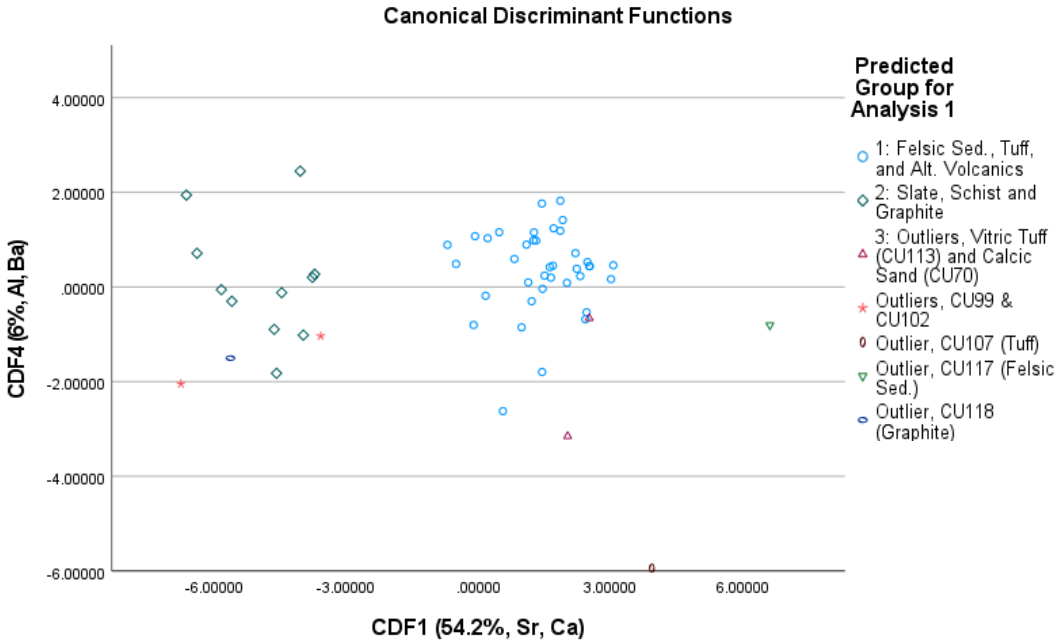

Figure D-8. Scatterplot of DF 2 by DF 3, Canchas Uckro DFA.

The Group 3 "outliers" are subsumed within the group 1 local assemblage in this analysis. This group is marked separately in the above scatterplot, as they are technologically distinct based on the results of petrographic analysis. Additional scatter plots highlight how well outliers are differentiated from other artifacts, perhaps with the exception of Group 7, an "outlier" graphite tempered sherd that more generally clusters with the mixed schist/slate/graphite group. They also demonstrate differentiation between technological traditions, including Group 1, associated with the local production practices (namely the felsic sediment tempered ware) and the schist/slate/graphite group likely associated with other nearby areas within the Conchucos region.

Conclusions:

The combined results of factor analysis, HCA, and DFA indicate that technological differences are geochemically identifiable, paralleling the observed technological categories identified during petrographic analysis. The Canchas Uckro assemblage is overall quite homogenous, forming a large cluster (Group 1) representing the intrusive volcanic-derived sediments, with a petrographically-identified tuff-tempered subgroup, potentially representing two distinct communities of practice.. Additionally, the altered volcanics group, associated with several unusual decorated sherds and believed to represent an imported technological tradition, is subsumed within this group.

Slate and graphite tempered sherds comprise Group 2. Slate is known in association with the Santa Carhuaz Formation, an outcrop of which forms the ridgeline just to the east of Canchas Uckro. Though this material was potentially "locally available", these sherds are quite coarsely made, quite rare within the overall assemblage, and seem to represent an altogether different *chaîne opératoire*, which points to an origin from another part of the Conchucos Region.

The pXRF data also highlight several consistent outliers and sub-groups. These particular pieces represent unique and rare materials within the overall assemblage and likely represent trade wares from yet undetermined sources. One potentially non-local cluster, tempered with altered volcanic

rock fragments, notably corresponds to many of the decorated sherds, some exhibiting Waira-jirca stylistic traits. These materials are geochemically and petrographically distinct from the general assemblage, suggesting they imports. These altered mineral grains, indicative of metamorphic alteration, would match with the reported geology of the Huánuco Basin, which consists of rocks associated with highly variable Neo-Proterozoic metasedimentary rocks, schists, gneisses of the Marañon Complex and Jurassic-aged granodiorite and tonalite (Quispesivana 1996).

Overall, these findings support the hypothesis that (1) technological practice was fairly limited for local ceramic production, comprised of one or two communities of practice with relatively minor potential variation in clay recipes. (2) The limited number of schist, slate, and graphite tempered sherds point to interaction within the Conchucos region, while a smaller subset of outlier sherds further indicate Canchas Uckro was enmeshed in the down-the-line trade relationships characteristic of the Early Horizon. However, the (3) hypotheses of a non-local origin for Waira-jirca wares is more complex, as some artifacts create a distinct geochemical sub-group, and others group with the dominant technological type, findings that are reflected and further supported by the petrographic findings. In sum, it is likely some of the Waira-jirca style sherds and vessels were imported to the site, while others were manufactured using raw materials local to Canchas Uckro.